Data Assimilation Experiments in the Gulf Stream Region: How Useful Are Satellite-Derived Surface Data for Nowcasting the Subsurface Fields?

TAL EZER AND GEORGE L. MELLOR

Program in Atmospheric and Oceanic Sciences, Princeton University, Princeton, New Jersey

(Manuscript received 3 March 1995, in final form 15 October 1995)

ABSTRACT

Satellite-derived surface data have become an important source of information for studies of the Gulf Stream system. The question of just how useful these datasets are for nowcasting the subsurface thermal fields, however, remains to be fully explored. Three types of surface data—sea surface temperature (SST), sea surface height (SSH), and Gulf Stream position (GSP)—are used here in a series of data assimilation experiments to test their usefulness when assimilated into a realistic primitive equation model. The U.S. Navy's analysis fields from the Optimal Thermal Interpolation System are used to simulate the surface data and to evaluate nowcast errors. Correlation factors between variations of the surface data and variations of the subsurface temperature are used to project the surface information into the deep ocean, using data and model error estimates and an optimal interpolation approach to blend model and observed fields.

While assimilation of each surface data source shows some skill in nowcasting the subsurface fields (i.e., reducing errors compared to a control case without assimilation), SSH data reduce errors more effectively in middepths (around 500 m), and SST data reduce errors more effectively in the upper layers (above 100 m). Assimilation of GSP is effective in nowcasting the deep Gulf Stream, while the model dynamics produce eddies that are not included in the GSP analysis. An attempt to optimally combine SST and SSH data in the assimilation shows an improved skill at all depths compared to assimilation of each set of data separately.

1. Introduction

With the development of more realistic numerical ocean models and the availability of satellite data in almost real time, the prospect of nowcasting and forecasting the ocean, as is done by numerical weather prediction models, becomes increasingly feasible. For example, an experimental coastal forecast system, based on the coupling of the Princeton Ocean Model (POM) used here to a mesoscale atmospheric model, has been running in a quasi-operational mode and producing daily forecasts since August 1993 (Aikman et al. 1996). In particular, recent interest is focused on attempts to nowcast and forecast the Gulf Stream system and to develop data assimilation techniques for ocean models (Holland and Malanotte-Rizzoli 1989; Robinson et al. 1989; Thompson and Schmitz 1989; White et al. 1990; Moore, 1991; Verron 1992; Mellor and Ezer 1991; Ezer et al. 1992, 1993; Ezer and Mellor 1994). There are two types of surface satellite data that may be useful for assimilation: sea surface temperature data (SST) from the Advanced Very High Resolution Radiometer (AVHRR)

and sea surface height data (SSH) from radar altimeters. A comparison of the two data types in the Gulf Stream region shows considerable differences due to differences in their spatial coverage and the interpolation methodology associated with the data assimilation system (Ezer et al. 1993).

Since satellite data provide only surface information, efficient data assimilation relies on the projection of the surface data into the deep ocean to obtain the three-dimensional oceanic fields. This can be done, for example, by using ''feature models'' for SST data (e.g., Robinson et al. 1989; Cummings and Ignaszewski 1991), or by using surface-to-subsurface correlations or deep adjustment techniques (e.g., Hurlburt et al. 1990; Carnes et al. 1990; Mellor and Ezer 1991; Haines 1991; Ezer and Mellor 1994; Rienecher and Adamec 1995) for altimetry data. Relying on surface insertion of data without the projection of the surface information to the deep layers may not be sufficient to constrain primitive equation models, as has been demonstrated recently in the study of Pinardi et al. (1995). Satellite data are especially useful in the identification of oceanic fronts such as those associated with the Gulf Stream system (Cornillon and Watts 1987; Cayula and Cornillon 1992; Glenn et al. 1991; Kelly 1991). There is a question, however, as to whether information on the Gulf Stream axis alone can be used in an automated data assimilation; to test this possibility is one of the goals here. Another

Corresponding author address: Dr. Tal Ezer, Program in Atmospheric and Oceanic Sciences, Princeton University, P.O. Box CN710, Sayre Hall, Princeton, NJ 08544-0710.
E-mail: ezar@splash.princeton.edu

goal is to see if the correlation technique, used for altimeter data by Mellor and Ezer (1991) and Ezer and Mellor (1994), can be also applied to SST data.

Many studies of data assimilation techniques often use identical twin experiments (i.e., model simulated data) to test the schemes. Here, however, instead of model-simulated data, analysis fields derived from the U.S. Navy's Optimum Thermal Interpolation System (OTIS) (Clancy et al. 1990, 1992; Cummings and Ignaszewski 1991) are used to initialize the model, to simulate the surface data (assuming the data are available at all surface grid points), and to evaluate nowcast errors. Therefore, it is presumed that in these experiments, the analysis fields represent the "true" ocean, where errors in the analysis fields themselves are neglected. This approach is advantageous over identical twin experiments since it tests the model adjustment to observed fields rather than its own, but at the same time still allows some quantitative evaluation of assimilation errors. Previous data assimilation studies have addressed the problem of errors associated with sampling altimeter data along satellite tracks (Kindle 1986; Holland and Malanotte-Rizzoli 1989; Mellor and Ezer 1991; Ezer et al. 1993; Ezer and Mellor 1994). Here, however, to evaluate the errors associated with the vertical projection of the surface data into the subsurface fields, sampling errors are neglected.

The data and the numerical model are described in section 2. In section 3 the data assimilation experiments are described, and in section 4 the assimilation methodology is presented. Assimilation results are discussed in section 5 and conclusions are offered in section 6.

2. Description of the numerical model and the OTIS data

a. The numerical ocean model

The POM is described by Blumberg and Mellor (1987) and Mellor (1992); it includes the turbulence submodel of Mellor and Yamada (1982) to provide vertical mixing parameters. Recent studies of the Gulf Stream system with the model focus on different dynamical aspects such as surface forcing and topographic effects (Ezer and Mellor 1992; Oey et al. 1992; Ezer 1994), as well as nowcast–forecast experiments and data assimilation studies (Mellor and Ezer 1991; Ezer et al. 1992, 1993; Ezer and Mellor 1994). The prognostic variables of the model are temperature T; salinity S; the free surface elevation η; velocities u, v, w; and the turbulent kinetic energy. The model has a bottom-following, sigma coordinate vertical system, with 15 levels in this application, and a curvilinear orthogonal, coastal following, horizontal grid with a typical resolution of 10 to 18 km in the Gulf Stream region; see Fig. 1 for the grid and the bottom topography.

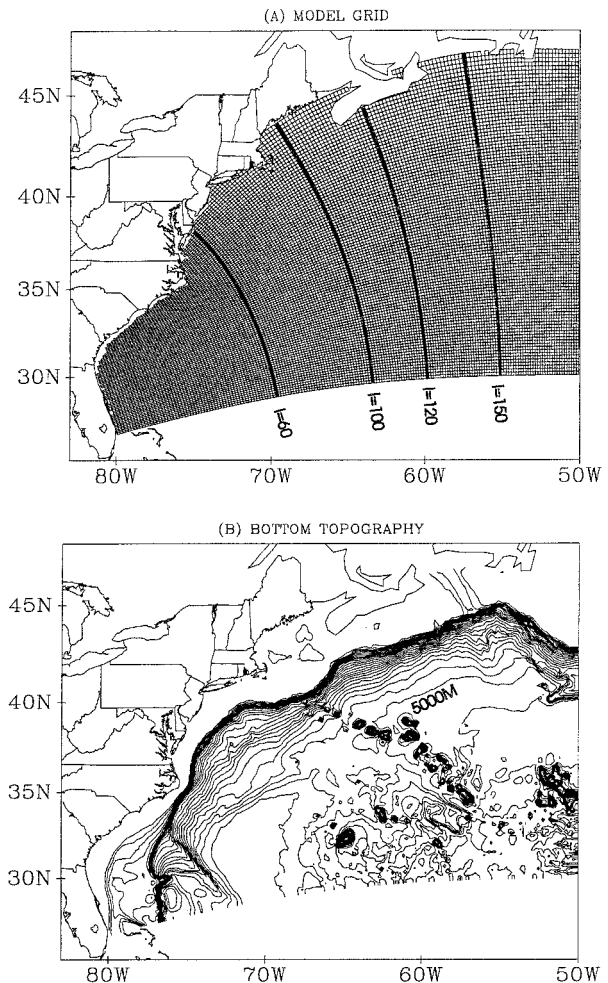The model was initialized with synoptic analysis tem-

FIG. 1. (a) The curvilinear orthogonal model grid; the indicated cross sections are referred to in Fig. 3. (b) The bottom topography of the model; the contour interval is 200 m. The actual boundary of the model domain is at the 10-m depth isobath.

perature and salinity data obtained from OTIS; then it was run for 1 week in a diagnostic mode (holding the temperature and the salinity fixed) to obtain the dynamically adjusted velocities and surface elevations. The total streamfunction on the boundaries is set according to basin-scale diagnostic calculations (Mellor et al. 1982) and observations. An inflow of 30 Sv (1 Sverdrup = 10^6 m^3 s^{-1}) is prescribed at the Florida Straits (the southwestern corner of the domain), inflow of 30-Sv slope water enter at the northern part of the eastern boundary, inflow of 40 Sv from the subtropical gyre enter at the southeastern and the southern boundaries, and 100-Sv Gulf Stream outflow are allowed to exit the domain on the eastern boundary between 38° and 39°N. Internal velocities on the open boundaries are governed by the Sommerfeld radiation conditions [see Mellor and Ezer (1991) and Ezer and Mellor (1992) for more details on the boundary conditions of the Gulf Stream model].

The surface forcing includes heat flux and wind stress fields obtained from the monthly climatologies of the Comprehensive Ocean–Atmosphere Data Set (COADS) analyzed by Oberhuber (1988); the formulation of the surface forcing in the model is described in detail by Ezer and Mellor (1992), who show the importance of the surface forcing in obtaining a realistic separation of the Gulf Stream at Cape Hatteras.

b. The OTIS analysis data

Analysis fields of temperature and salinity at a given time are obtained from OTIS. The global-scale system is described in detail by Clancy et al. (1990, 1992), and the regional high-resolution version of OTIS used here is described by Cummings and Ignaszewski (1991). Satellite infrared images are used to identify the Gulf Stream's north wall and rings. Then, feature models, describing the shape of the stream and rings, project the surface information into the deep layers, producing three-dimensional synthetic temperature and salinity data. The input data to OTIS includes the synthetic data, multi-channel sea surface temperature (MCSST) data, climatological data, and expendable bathythermograph (XBT) data; these data are used to produce the three-dimensional thermal field via an optimal interpolation method. The data is projected on a $0.2° \times 0.2°$ horizontal grid and 34 vertical levels. The OTIS model has been run at the Center for Ocean and Atmospheric Modeling (COAM) of the University of Southern Mississippi using high quality data prepared especially for the Data Assimilation and Model Evaluation Experiments (DA-MEEs) (Willems et al. 1994).

The analysis temperature at 500 m during the period in which the data assimilation experiments were performed are shown in Fig. 2; these data are now used to describe some of the dynamical processes and the observed evolution of the Gulf Stream system during this period. At this depth, the temperature gradient across the Gulf Stream front is maximum. Although some of the deficiencies of the OTIS analysis, like a lack of small-scale variability (Ezer et al. 1993) and too smooth fronts, are obvious, these fields are still useful to study changes in the meandering stream and its associated eddies. Model simulations may correct, however, some of these deficiencies. The study period is characterized by several important events (Fig. 2). A strong warm core eddy developed at 40°N, 65°W on 11 May was observed drifting westward during the entire period. Then, the wide meander trough, observed at the first 3 weeks, shed a cold core eddy at 57°W on 25 May. For the next 3 weeks the Gulf Stream had little meandering activity until 22 June when a meander crest at 63°W and a sharp meander trough at 60°W developed due to the interaction of the stream with warm and cold core eddies, respectively. We will try to evaluate later, if assimilation of surface information alone is sufficient to predict these Gulf Stream processes.

The sea surface height associated with each of these OTIS fields is obtained from the model surface elevation after a week of diagnostic calculation (i.e., holding T and S unchanged and equal to those of each analysis). The diagnostic calculation gives similar results to dynamic height calculations, except that a level of no motion needs not be specified, and SSH can be calculated in shallow regions. Examples of SSH cross sections (see Fig. 1a for their location) are shown in Fig. 3 for the period 4 May–4 July 1988; they show about a 1-m change in sea level across the Gulf Stream. At $I = 60$, in the western portion of the stream, only little change is observed during this period. At $I = 100$, just west of the New England Seamount Chain, the stream position does not change by much, but evidence of warm core eddies is seen in this section. At $I = 120$, across the seamount chain, large changes in the stream's position by as much as 400 km is observed during this 2-month period. The last section at $I = 150$ shows more variations in the stream than the western sections. Recently, numerical simulations of Ezer (1994) demonstrate the strong influence that the seamount chain has on the Gulf Stream meanders; some of these changes in the Gulf Stream dynamics have been observed before and are also evident in Fig. 3. When Gulf Stream axis locations are assimilated, the above spatial changes in the SSH cross sections will be taken into account in the scheme described below.

3. The data assimilation experiments

Five 2-month-long experiments are performed, starting from the same initial conditions, the OTIS field on 4 May 1988 (Fig. 2), forced by the same climatological COADS winds, and with the same lateral boundary conditions. In each experiment, different surface data are assimilated except for the control case without assimilation (see Table 1 for the detail of the assimilation and the surface boundary conditions used in each experiment). The runs start with 7 days of diagnostic calculations (i.e., holding T and S fixed and equal to the initial condition) for dynamic adjustment, followed by 63 days of prognostic calculations. The surface data (SSH, SST, and GSP) are assimilated once a day; the data are linearly interpolated from the weekly analyses to each day. Evaluation of the assimilation of different surface data is done by comparing the subsurface fields from each experiment to the corresponding OTIS fields. The term "nowcast," used here and throughout the paper, refers to data assimilation experiments (i.e., experiments 2 to 5), while the term "forecast" refers to calculations without assimilation (i.e., experiment 1). The latter depends on the initial condition and the model predictive skill (as in Ezer et al. 1992); the former depends also on the assimilated data.
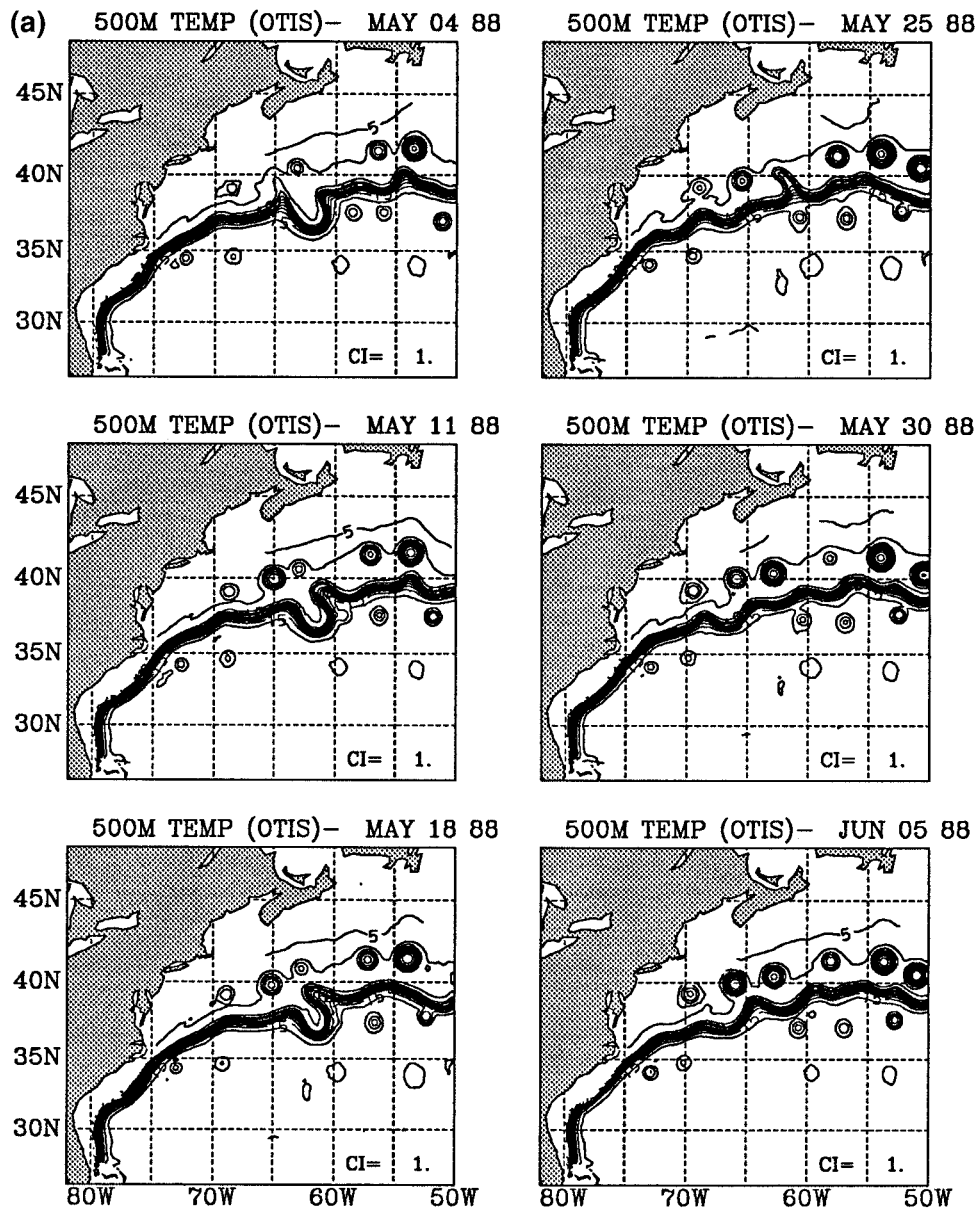
FIG. 2. The temperature at 500 m obtained from the OTIS analysis for 4 May to 4 July 1988. Contour interval is 1°C.

4. The data assimilation scheme

a. Assimilation methodology

The assimilation scheme is based on the methodology developed for altimeter data by Mellor and Ezer (1991) and Ezer and Mellor (1994) with some modifications. Data errors in the analysis fields and in the identification of the Gulf Stream axis are neglected here; they will be discussed later. Because the salinity fields in OTIS are much less reliable than temperature fields, the assimilation involves only subsurface temperature, while salinities are calculated as a predictive

variable of the model. However, the formulation for updating salinity fields is similar to that of temperature fields (Mellor and Ezer 1991).

The main thrust of the scheme is the use of predetermined surface–subsurface correlation coefficients, $C_{TT}(x, y, z)$, $C_{T\eta}(x, y, z)$, and correlation factors, $F_{TT}(x, y, z)$, $F_{T\eta}(x, y, z)$ (properties derived from correlations between surface and subsurface fields are indicated by two subscripts: the first one represents the subsurface variable and the second one represents the surface variable); they are defined by
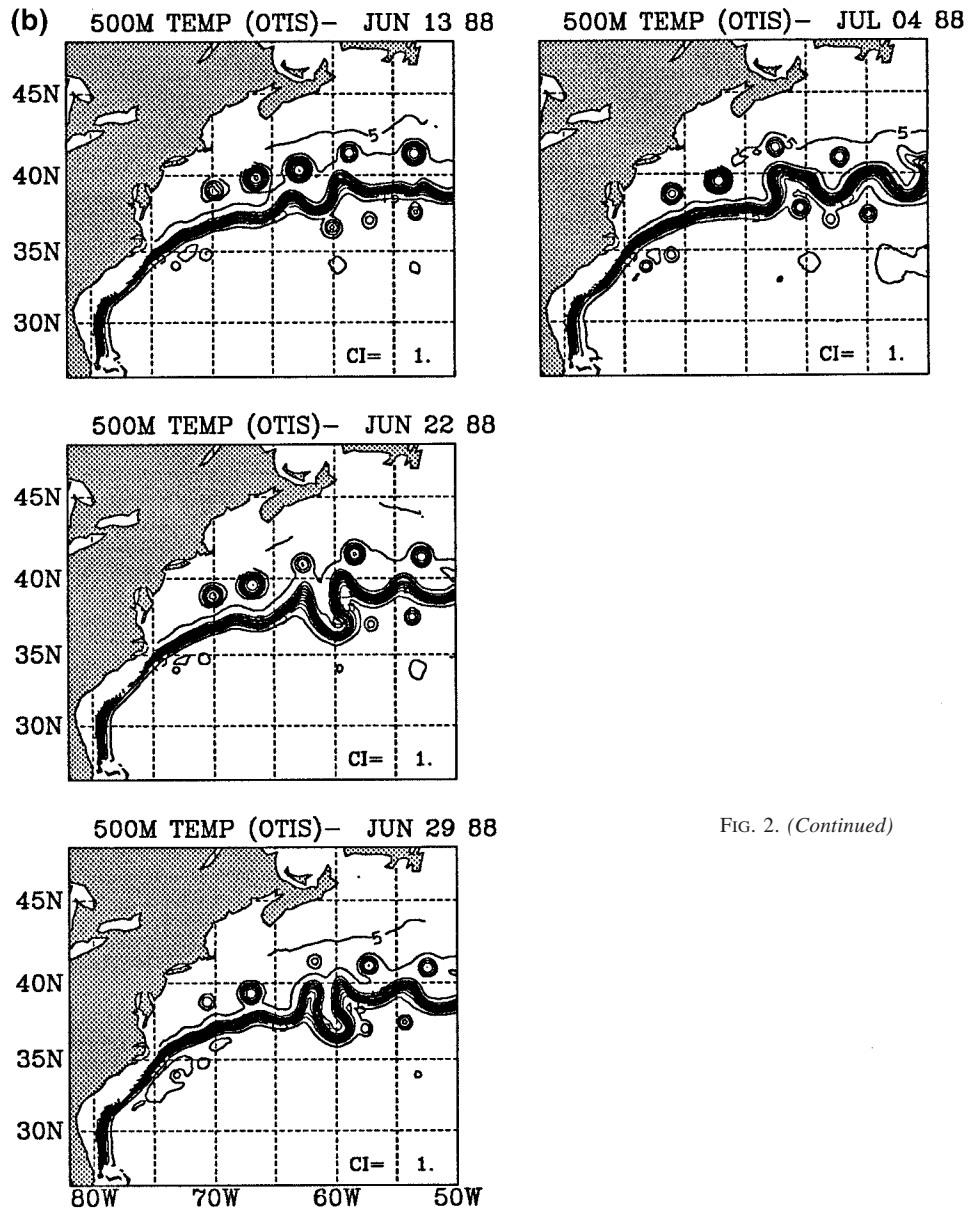
(b) 500M TEMP (OTIS)- JUN 13 88

500M TEMP (OTIS)- JUL 04 88

500M TEMP (OTIS)- JUN 22 88

FIG. 2. *(Continued)*

500M TEMP (OTIS)- JUN 29 88

$$C_{TT} = \frac{\overline{(\delta T \delta T^{\text{surf}})}}{[\overline{(\delta T)^2}\, \overline{(\delta T^{\text{surf}})^2}\,]^{1/2}}, \qquad F_{TT} = \frac{\overline{(\delta T \delta T^{\text{surf}})}}{\overline{(\delta T^{\text{surf}})^2}}, \quad (1\text{a,b})$$

$$C_{T\eta} = \frac{\overline{(\delta T \delta \eta)}}{[\overline{(\delta T)^2}\, \overline{(\delta \eta)^2}\,]^{1/2}}, \qquad F_{T\eta} = \frac{\overline{(\delta T \delta \eta)}}{\overline{(\delta \eta)^2}}, \qquad (2\text{a,b})$$

relating variations of the surface temperature anomaly $\delta T^{\text{surf}}(x, y)$ and surface elevation anomaly $\delta\eta(x, y)$ to variations of temperature anomaly at depth $\delta T(x, y, z)$; overbars indicate a time average. These coefficients are calculated here from the statistics of the OTIS data (using analysis fields from 1987 and 1988) but, as shown in Ezer and Mellor (1994), these correlations are quite similar to those obtained from the model statistics. Higher correlations are obtained in the vicinity

of the Gulf Stream and lower values are found in shallow regions and far from the Gulf Stream [the vertical distribution of these coefficients are shown later; see also Mellor and Ezer (1991) for the spatial distribution]. At each assimilation time, the analysis temperature, which is used as initial condition for the next 1-day forecast until new data are assimilated, is derived from the model first-guess field $T^m(x, y, z)$ and the "observed" subsurface temperature field $T^{\text{obs}}(x, y, z)$, according to

$$T^a = T^m + P(T^{\text{obs}} - T^m). \qquad (3)$$

The calculation of the observed subsurface temperature from the surface data and the calculation of the weights

SSH MAY 4 − JUL 4 1988 AT I= 60

SSH MAY 4 − JUL 4 1988 AT I= 100

SSH MAY 4 − JUL 4 1988 AT I= 120

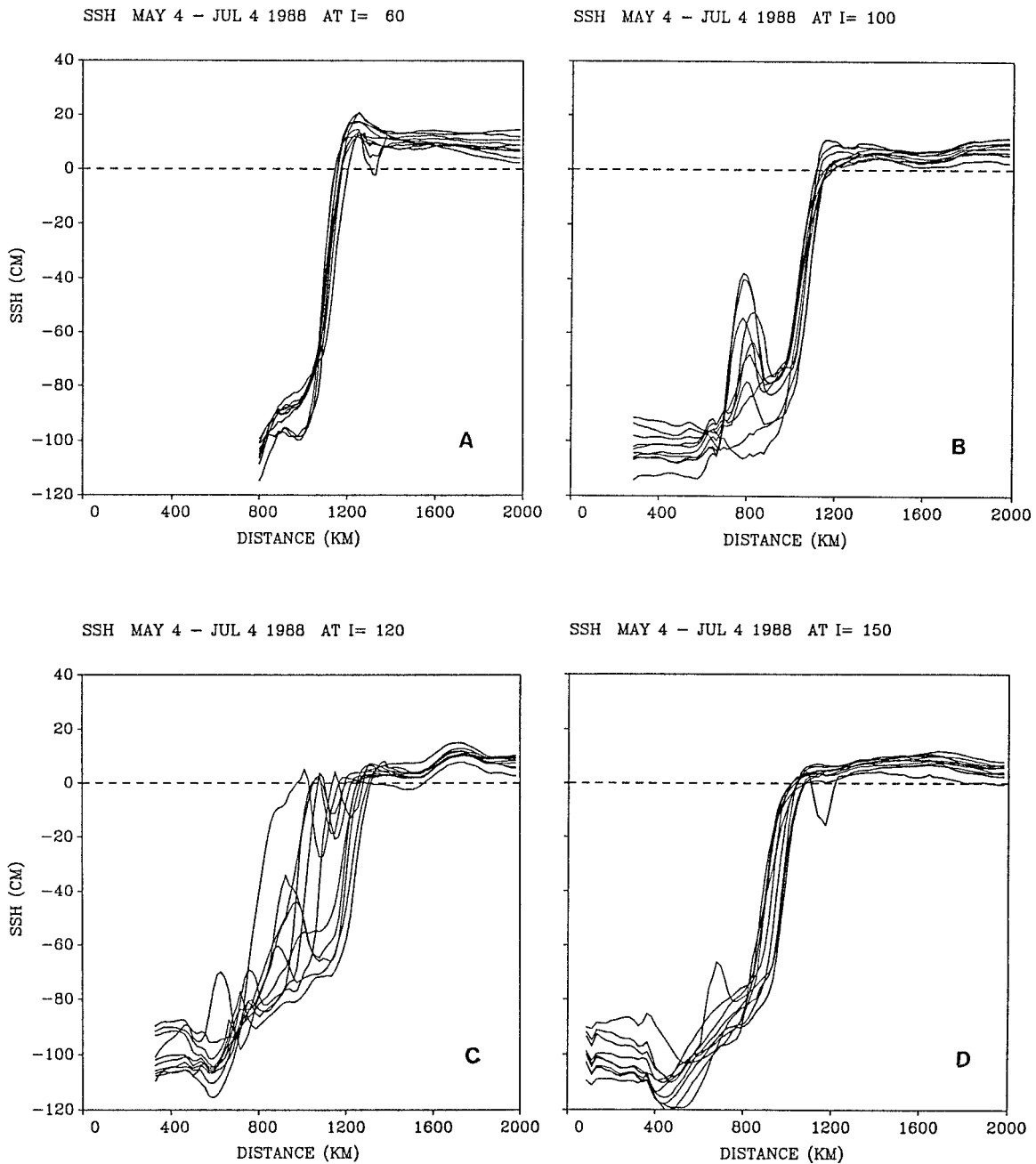SSH MAY 4 − JUL 4 1988 AT I= 150

FIG. 3. Sea surface height cross sections obtained from diagnostic calculations with the OTIS data of Fig. 2. The cross sections are indicated in Fig. 1; they are along the model grid at (a) $I = 60$, (b) $I = 100$, (c) $I = 120$, and (d) $I = 150$.

$P(x, y, z)$ for each dataset are described below. Errors associated with the imperfect surface–subsurface correlations (1a) and (2a) are taken into account in the derivation of the optimal weights. However, errors associated with measurement inaccuracies and with horizontal interpolations are neglected in this study [see Ezer and Mellor (1994) for the details on how such errors can be taken into account in this scheme]. Since the focus here is on the region where most of the Gulf Stream variations occur, data are not assimilated upstream of Cape Hatteras and in regions shallower than 1000 m.

b. Assimilation of SST data

In the case of assimilation of SST data, the observed subsurface temperature at each assimilation time in (3)

TABLE 1. The data type used for assimilation and for surface boundary condition for each experiment. In experiments 2, 4, and 5, the SST data, used for surface boundary condition, are the same as the OTIS-derived SST used for assimilation in experiments 2 and 4. The SST used as boundary condition in experiment 3 is calculated from Eq. (5a) (assuming that SST is not available, only SSH).

Experiment	Data assimilated	Surface boundary condition
1	No assimilation	Heat flux (COADS)
2	SST	SST (OTIS)
3	SSH	SST [Eq. (5a)]
4	SST + SSH	SST (OTIS)
5	GSP	SST (OTIS)

is calculated from the anomaly of the observed SST, δT^{surf}, according to

$$T_{TT}^{\text{obs}} = \overline{T} + F_{TT}\delta T^{\text{surf}}, \tag{4a}$$

where $\overline{T}$ is the seasonal (May to July) mean temperature and the weights in (3) are

$$P_{TT} = C_{\text{fg}}(1 + C_{\text{fg}} - C_{TT}^2)^{-1}. \tag{4b}$$

The derivation of (4b) from standard optimal interpolation methodology can be found in appendix A in Mellor and Ezer (1991). The first-guess error parameter $0 < C_{\text{fg}} < C^{\text{max}}$ reaches its maximum theoretical value of $C^{\text{max}} = 2$ if no assimilation is done for a period comparable to the model error growth timescale ($\tau \approx 20$ days near the Gulf Stream). While in the identical twin experiments of Mellor and Ezer (1991) C_{fg} has been chosen as a constant based on sensitivity experiments, in the study of Ezer and Mellor (1994), using real altimeter data, $C_{\text{fg}}(x, y, t)$ has been calculated using a more sophisticated formulation for model error growth and data error estimates. However, for our simple case of a uniform data coverage (i.e., at all surface grid points) and a constant assimilation time step ($\Delta t = 1$ day), this parameter can be taken as a constant $C_{\text{fg}} = (C^{\text{max}}\Delta t/\tau) = 0.1$. In the sensitivity studies of Mellor and Ezer (1991) C_{fg} values between 0.1 and 1 have been tested with relatively small effects on the assimilation results. If a perfect surface–subsurface correlations exist and data errors are neglected, the weights are independent of C_{fg} and the model fields are simply replaced by the observed fields. On the other hand, in regions of poor correlation (e.g., far from the Gulf Stream) little weight is given to the observations, thus model dynamics dominate.

c. Assimilation of SSH data

Assimilation of SSH data is similar to assimilation of SST, where the subsurface temperature at each assimilation time is calculated from the anomaly of the observed SSH, $\delta\eta = (\eta^{\text{obs}} - \overline{\eta})$ according to

$$T_{T\eta}^{\text{obs}} = \overline{T} + F_{T\eta}\delta\eta, \tag{5a}$$

and the weights in (3) are

$$P_{T\eta} = C_{\text{fg}}(1 + C_{\text{fg}} - C_{T\eta}^2)^{-1}. \tag{5b}$$

In our case, the observed SSH fields are obtained from diagnostic calculation using the density field of each OTIS analysis. However, altimeter data (interpolated from satellite tracks into the model grid) can be used the same way, as has been done in Ezer and Mellor (1994). In the latter case, additional errors associated with the horizontal interpolation and with altimeter errors are taken into account when the optimal interpolation is used to obtain $\delta\eta$ on model grid from the altimeter data along satellite tracks.

d. Assimilation of SST and SSH data

We try now to optimally combine two types of data sources: SST and SSH. Thus, instead of (3), the analysis temperature at each assimilation step is calculated according to

$$T^a = T^m + P_{TT}(T_{TT}^{\text{obs}} - T^m) + P_{T\eta}(T_{T\eta}^{\text{obs}} - T^m), \tag{6}$$

where the weights and the subsurface observed fields are from (4) and (5). The optimal combination takes into account the fact that the errors in the projection of surface information to the subsurface fields depend on the square of the correlation coefficient [i.e., (4b) (5b); see also Mellor and Ezer (1991) for the derivation of these errors]. Other options of combining SST and SSH data, such as using SST for the upper layers and using SSH for the deep layers, have been tested before (Ezer et al. 1991) but did not indicate any improved skill over (6).

e. Assimilation of GSP data

The surface location of the Gulf Stream axis can be obtained from satellite SST data (Cornillon and Watts 1987; Cayula and Cornillon 1992) or from satellite altimetry data (Glenn et al. 1991; Kelly 1991) with an accuracy of about 10 to 20 km. Here, however, we neglect those errors since the axis is obtained directly from the analysis SSH (from diagnostic calculations). The Gulf Stream axis is defined here as the location of the maximum gradient in SSH. At each assimilation step, the observed SSH anomaly in (5a) is replaced by the artificial SSH obtained as follows:

$$\eta^{\text{obs}}(x, y) = \overline{\eta}[x, (y - y_{\text{axis}}^{\text{obs}} + y_{\text{axis}}^{\text{mean}})], \tag{7}$$

where x and y are the i and j curvilinear model coordinates that are approximately in the along-stream and the across-stream directions, respectively. The only information used in (7) is the observed position of the Gulf Stream axis $y_{\text{axis}}^{\text{obs}}$ and the mean SSH cross section at each x. Note that for each location along the Gulf Stream, a different mean profile is used, taking into account the downstream change in the Gulf Stream strength and variability (Fig. 3). After this SSH is obtained in (7), the assimilation of the subsurface tem-
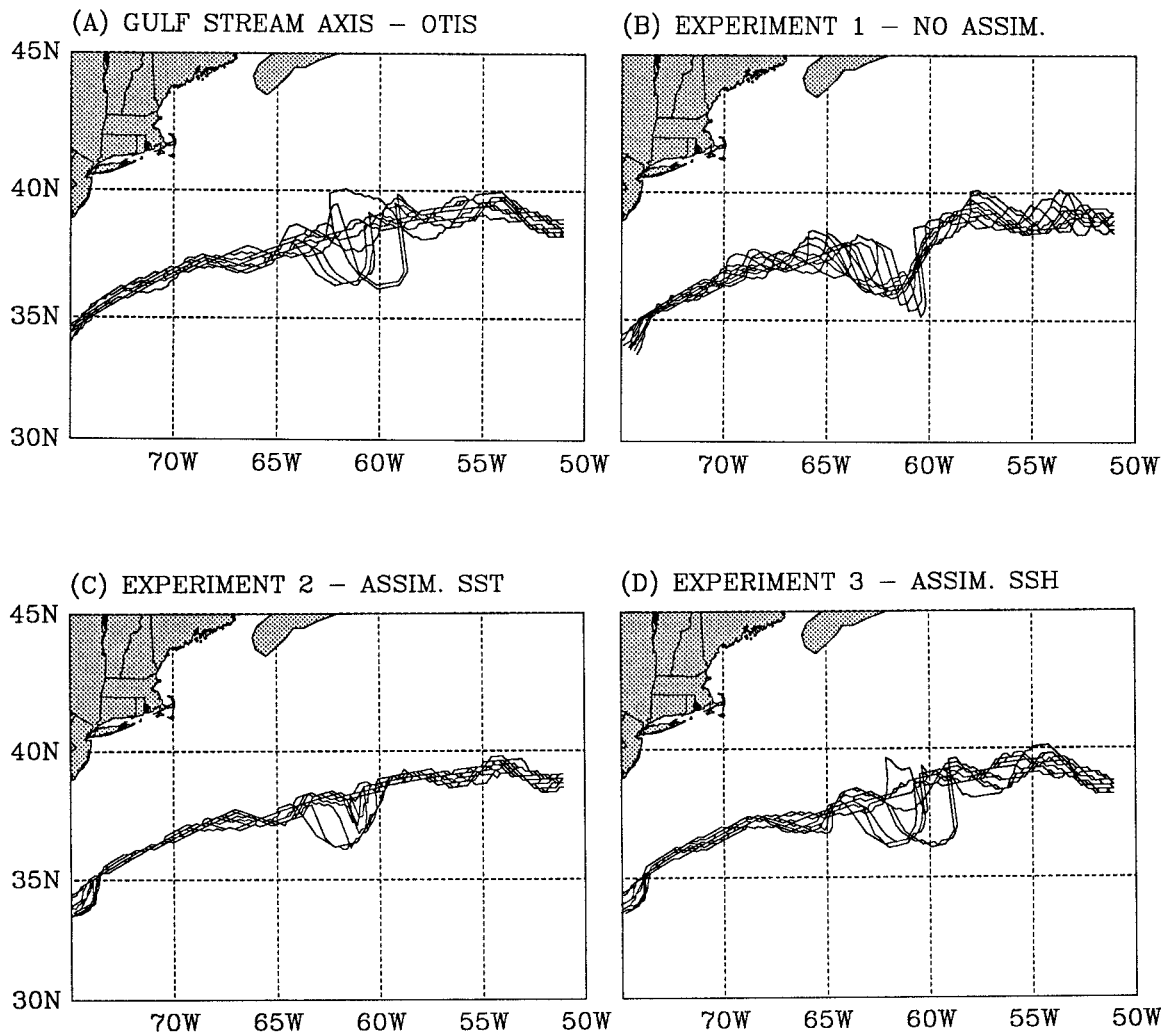
FIG. 4. The Gulf Stream axis, derived from the 12°C contour at 500 m, as obtained from (a) the OTIS data, (b) model forecast without data assimilation, (c) model nowcast with assimilation of SST data, and (d) model nowcast with assimilation of SSH data.

perature is done as in the case of assimilation of SSH using (3) and (5). The use of GSP only does not include any information on eddies and recirculation; testing will determine whether the model's dynamics can fill in this missing information.

5. Assimilation results

Different aspects of the fields obtained from the data assimilation experiments are evaluated and compared with the forecast (experiment 1) to evaluate the type of data that are most useful in improving the nowcast. Nowcast skill is defined here as the ability to reduce errors compared with the pure forecast without assimilation; nowcast errors are the differences between the model and the analysis fields, neglecting, at this time, possible errors in the analysis. We first discuss experiments 2, 3, and 5 in which only one type of data (SST,

SSH, or GSP) are assimilated, and then experiment 4 where two types of data (SST and SSH) are combined.

A common definition of the subsurface Gulf Stream axis is the 12°C contour at 500-m depth. Figures 4b, 4c, and 4d compare the axis obtained from experiments 1, 2, and 3 to that obtained from the OTIS analysis (Fig. 4a). The forecast axes without assimilation (Fig. 4b) is clearly much different than the observed axes (Fig. 4a); this result is expected since in this region a limited forecast skill exists only for a period of 2–3 weeks (Mellor and Ezer 1991; Ezer et al. 1992). Although some improvement in the prediction of the variations of the stream are seen when SST is assimilated (Fig. 4c), clear deficiencies, like the absent of the large meanders at 60°W, are evident. The axes obtained from assimilation of SSH (Fig. 4d) are almost identical to the observed axes (Fig. 4a) during this period, demonstrating the fact that surface height fields contain

(A) 500M TEMP. – OTIS

(B) EXPERIMENT 1 – NO ASSIM.

(C) EXPERIMENT 2 – ASSIM. SST

(D) EXPERIMENT 3 – ASSIM. SSH

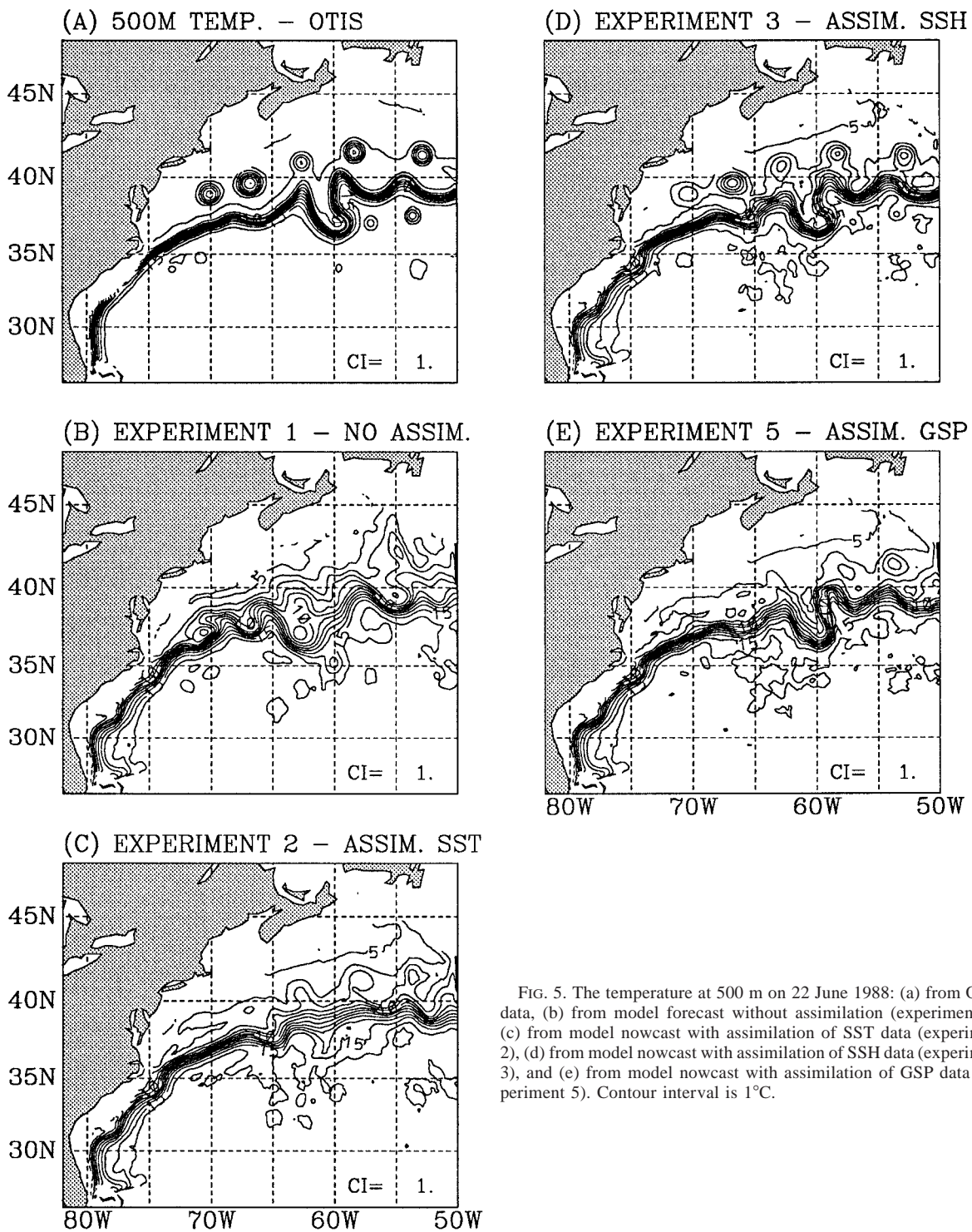## (E) EXPERIMENT 5 – ASSIM. GSP

FIG. 5. The temperature at 500 m on 22 June 1988: (a) from OTIS data, (b) from model forecast without assimilation (experiment 1), (c) from model nowcast with assimilation of SST data (experiment 2), (d) from model nowcast with assimilation of SSH data (experiment 3), and (e) from model nowcast with assimilation of GSP data (experiment 5). Contour interval is 1°C.

most of the information about the location of the sub-surface Gulf Stream front.

We now look in more detail at one of the events in the development of the Gulf Stream during this period—the large meander developed in the middle of June 1988 at 60°W due to a stream–eddy interaction (see

Fig. 2 and the discussion in section 2b). The forecast without assimilation (Fig. 5b) does predict a meander trough at this time (22 June 1988); however, it is much wider than that observed (Fig. 5a) and is located westward of the observed location. Warm core and cold core eddies predicted by the forecast at 55° and 60°W,
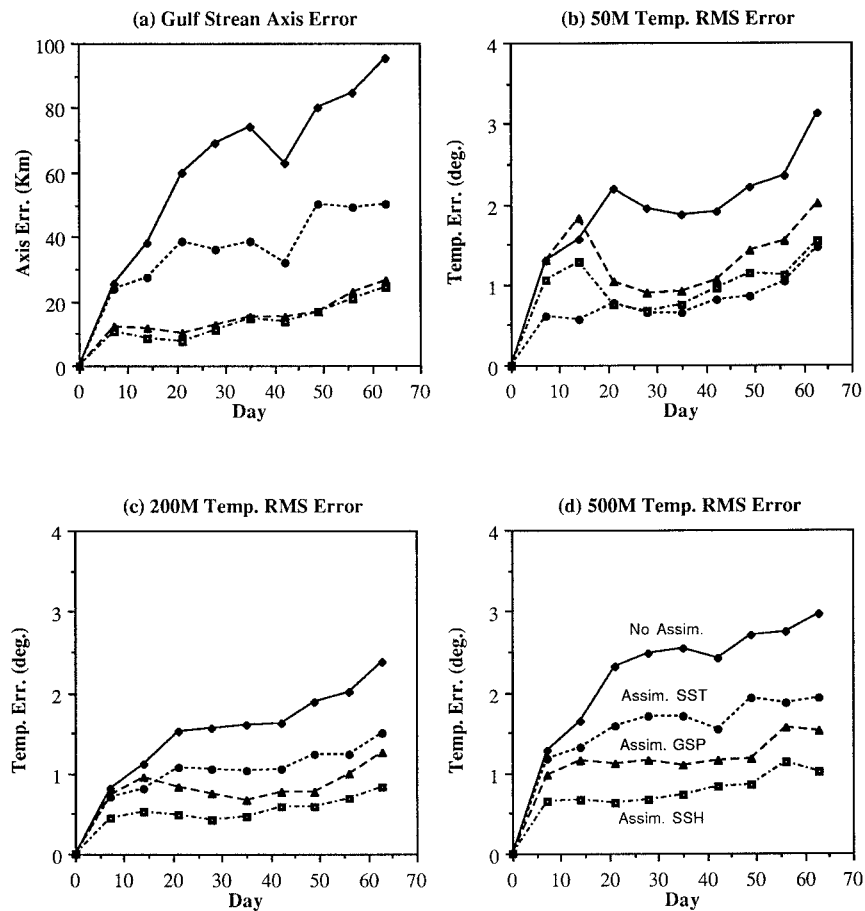
FIG. 6. Evaluation of forecast and nowcast errors relative to OTIS data. The solid line indicates the forecast without assimilation; the short dashed line indicates assimilation of SST data; dashed and dotted line indicates assimilation of SSH data; and long dashed line indicates assimilation of surface Gulf Stream position data. (a) Error in the subsurface Gulf Stream axis (the 12°C contour at 500 m), (b) rms errors in temperature at 50 m, (c) rms errors in temperature at 200 m, and (d) rms errors in temperature at 500 m.

respectively, are not observed, whereas the observed eddies are not predicted. Since this event occurs some 7 weeks after initialization, forecast skill is not expected for such a long period. Assimilation of SST improves the mean location of the stream somewhat compared to the forecast without assimilation. However, the meander discussed above is missing from the nowcast (see Fig. 5c). Note, however, that some of the observed eddies are produced (though with reduced intensity) by the nowcast since SST data contain some of their signature. Generally, assimilation of SST alone does not seem to be able to capture this meander event. The nowcast based on assimilation of SSH (Fig. 5d) seems to capture the observed Gulf Stream meanders and eddies very well, including the shape of the large meander at 60°W. Assimilation of surface GSP, on the other hand (Fig. 5e), produces good nowcasts of the subsurface position of the stream. Although assimilation of GSP does not include any information about

eddies, some eddies are produced since model dynamics are involved in the nowcast.

We now evaluate, quantitatively, the nowcast errors and consequently the skill of each of the assimilation experiments. The nowcast errors are compared here to the forecast errors; if the scheme has some skill, nowcast errors should be smaller than forecast errors. Only the region downstream of Cape Hatteras and in the vicinity of the Gulf Stream (about 5° north and south of the stream, excluding the shallow regions where water depth is less then 2000 m) are included in the analysis of errors.

The errors in the subsurface Gulf Stream axis (i.e., the 12°C contour at 500 m) averaged along the stream downstream of Cape Hatteras are shown in Fig. 6a. Although assimilation of SST alone reduces the error compared to the forecast without assimilation by about 50%, it is the least effective source of information for nowcasting the position of the stream. Assimilation of
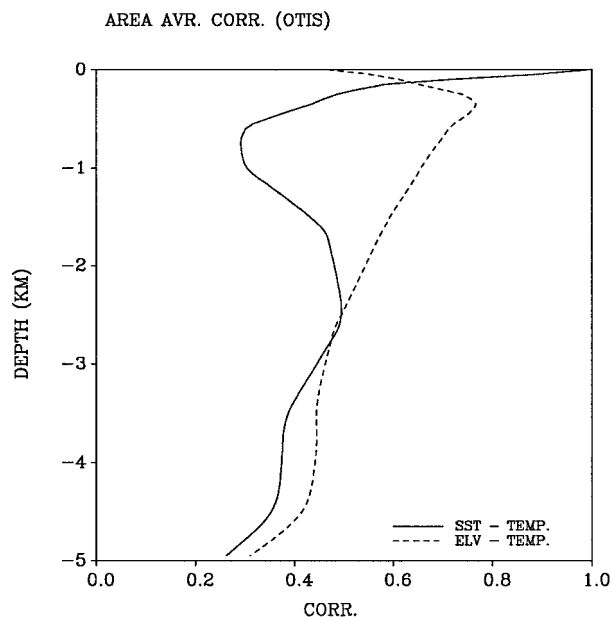
AREA AVR. CORR. (OTIS)

FIG. 7. Area-averaged profiles of the correlation coefficients C_{TT} (solid line) and $C_{T\eta}$ (dashed line). The correlations have been calculated from the OTIS fields for May to July 1987 and 1988. Only the area downstream of Cape Hatteras and where water depth is greater than 1000 m has been used in the calculations.

TEMPERATURE ERRORS

FIG. 8. Root-mean-square errors (°C) (averaged over time, excluding the first 2 weeks of the experiments), are shown as a function of depth for the different experiments: no assimilation (heavy solid line), assimilation of SST (dotted line), assimilation of SSH (dashed line), and assimilation of both SST and SSH (thin solid line). The area used in the calculations is as in Fig. 7.

either GSP or SSH reduces the forecast error by as much as 80% to less then 20 km after 2 months. The error in the nowcast of subsurface axis when using surface data comes from the errors in the surface–subsurface correlations; similar errors were obtained before in the identical twin experiments of Mellor and Ezer (1991), but they have also indicated errors that are about twice as large when altimeter data are sampled along Geosat tracks compared with a case where a complete coverage of SSH was available. We now evaluate the errors in the temperature field at different depth by calculating the rms errors over the region discussed before. At a depth of 50 m, assimilation of SST data yields somewhat better skill than the other surface data, whereas assimilation of GSP has the least skill. Since the model has a mixed layer dynamics, variations in the mixed layer temperature are associated more with changes in the surface temperature than in changes in surface height. For levels above 50-m depth, the skill of SST assimilation increases almost linearly with decreasing distance from the surface (at the surface itself, nowcast errors are zero by definition since $F_{TT} = 1$). However, at deeper levels (e.g., at 200 and 500 m, Figs. 6c and 6d) SST is the least effective data, while SSH is the most effective source of data for assimilation. Even the GSP, which contains much less information than SST data, is quite efficient, more than SST, in nowcasting the deep temperature field. This is due to the fact that variations of temperature in this region are dominated by the fluctuations of the Gulf Stream; thus, the surface position
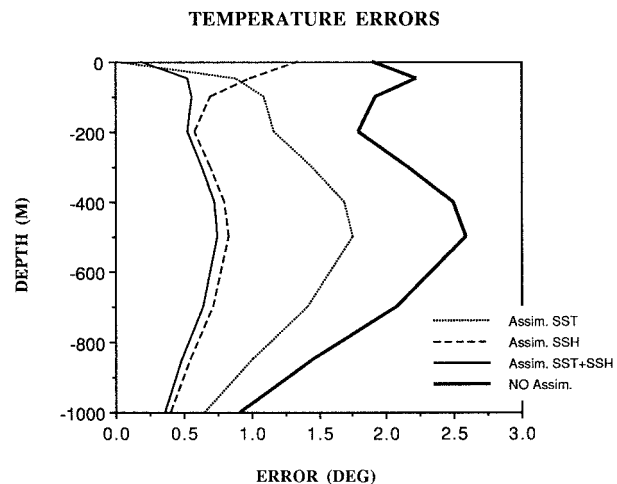
of the Gulf Stream contains most of the information needed to construct the subsurface temperature fields.

While all nowcasts show some skill (i.e., nowcast errors smaller than forecast errors, Fig. 6), the vertical distribution of the nowcast errors is different for each type of surface data. In particular, while SST is useful for nowcast fields in the upper ocean, SSH and GSP are more useful for nowcasting the deep Gulf Stream. This difference is explained by the vertical distribution of the area-averaged correlation coefficients shown in Fig. 7. The SSH–T correlations are maximum around 500 m, where the temperature gradients across the Gulf Stream are maximum, with decreasing correlations below and above this depth. The SST–T correlations are maximum, of course, at the surface with a minimum just below the main thermocline around 1000-m depth. Only in the upper 100 m are correlations of temperature with SST larger than correlations with SSH. The above differences between the effectiveness of different surface data lead to the hypothesis that using a combination of different datasets will improve the assimilation skill; testing this hypothesis is the main purpose of experiment 5, which is discussed below.

Indeed, the average errors as a function of depth, shown in Fig. 8, indicate that assimilation of SST and SSH together yields smaller errors at all depths than assimilation of each data alone. In the upper layers where SST–T correlations are higher (Fig. 7), the combined assimilation relies more on SST data, while in the deep layers where SSH–T correlations are higher, it relies more on SSH data as the weights in (6) depend on the square of these correlation coefficients. Even in the deep layers, skill is slightly improved over assimilation

of SSH alone due to the additional information included in the SST data.

6. Conclusions

Three types of surface data that can be obtained from satellite observations, SSH, SST, and GSP, are evaluated here for their usefulness in improving the nowcast skill of a data assimilation system of the Gulf Stream region. The data assimilation system is based on a realistic ocean model and the projection of surface data into the deep layers using an optimal interpolation approach and predetermined surface-to-subsurface correlations. The interpolation takes into account errors in the projection of surface data into the deep ocean, but neglects sampling errors in the data.

Since the correlation of SSH with the subsurface temperature is maximum at about a 500-m depth (Fig. 7) where the thermal gradients across the Gulf Stream are maximum, SSH data is the most efficient source of information (when neglecting sampling errors) for nowcasting the evolution of the stream and its associated eddies. In the upper layers (above 100-m depth), however, SSH do not correlate well with the temperature field (probably due to the mixed layer dynamics) and thus SST seems to be the more efficient source of data. Note that experiments (not shown here) where SST data is used only as a surface thermal boundary condition without the vertical projection show very little skill compared to the forecast without any use of data. While large-scale general circulation ocean models are often driven by observed SST, this approach does not seem to be sufficient for the short timescales typical for the Gulf Stream. Assimilation of GSP data by converting the Gulf Stream position into an artificial SSH field and then using SSH–T correlation has been shown to be a very effective way to nowcast the evolution of the deep stream. In this case, since no data is used for the eddy field, the model dynamics may help to predict the formation of new eddies or the drifting of old eddies that existed in the analysis used for the initial condition.

Since all three data types are now obtained routinely from earth observing satellites, they can be combined in an optimal way in a nowcast–forecast system that will provide important information to predict and study the evolution and the dynamics of the Gulf Stream system. The experiment where SST and SSH are assimilated together does show an improved skill at all depths compared to assimilation of each data alone.

REFERENCES

Aikman, F., G. L. Mellor, D. Rao, T. Ezer, D. Shenin, K. Bosley, and P. Chen, 1996: Toward an operational nowcast/forecast system for the U.S. east coast. *Modern Approaches to Data Assimilation in Ocean Modeling,* P. Malanotte-Rizzoli, Ed., Elsevier, 347–376.

Blumberg, A. F., and G. L. Mellor, 1987: A description of a three-dimensional coastal ocean circulation model. *Three-Dimensional Coastal Ocean Models,* N. Heaps, Ed., Vol. 4, American Geophysical Union, 1–16.

Carnes, M. R., J. L. Mitchell, and P. W. deWitt, 1990: Synthetic temperature profiles derived from Geosat altimetry: Comparison with air-dropped expendable bathythermograph profiles. *J. Geophys. Res.,* **95,** 17 979–17 992.

Cayula, J. F., and P. Cornillon, 1992: Edge detection algorithm for SST images. *J. Atmos. Oceanic Technol.,* **9,** 67–80.

Clancy, R. M., P. A. Phoebus, and K. D. Pollak, 1990: An operational global-scale ocean thermal analysis system. *J. Atmos. Oceanic Technol.,* **7,** 233–254.

——, J. M. Harding, K. D. Pollak, and P. May, 1992: Quantification of improvements in an operational global-scale ocean thermal analysis system. *J. Atmos. Oceanic Technol.,* **9,** 55–65.

Cornillon, P., and D. R. Watts, 1987: Satellite thermal infrared and inverted echo sounder determination of the Gulf Stream northern edge. *J. Atmos. Oceanic Technol.,* **4,** 712–723.

Cummings, J. A., and M. J. Ignaszewski, 1991: The Fleet Numerical Oceanography Center regional ocean analysis system. *MTS '91, Proc. Marine Technology Society,* New Orleans, LA, 1123–1129.

Ezer, T., 1994: On the interaction between the Gulf Stream and the New England Seamounts Chain. *J. Phys. Oceanogr.,* **24,** 191–204.

——, and G. L. Mellor, 1992: A numerical study of the variability and the separation of the Gulf Stream, induced by surface atmospheric forcing and lateral boundary flows. *J. Phys. Oceanogr.,* **22,** 660–682.

——, and ——, 1994: Continuous assimilation of Geosat altimeter data into a three-dimensional primitive equation Gulf Stream model. *J. Phys. Oceanogr.,* **24,** 832–847.

——, ——, and D.-S. Ko, 1991: Nowcasting the Gulf Stream structure with a primitive equation model and assimilation of altimetry and SST data. *MTS '91, Proc. Marine Technology Society,* New Orleans, LA, 236–241.

——, D. S. Ko, and G. L. Mellor, 1992: Modeling and forecasting the Gulf Stream. *Oceanic and Atmospheric Nowcasting and Forecasting,* D. L. Durham and J. K. Lewis, Eds., Vol. 26(2), Marine Technological Society, 5–14.

——, G. L. Mellor, D.-S. Ko, and Z. Sirkes, 1993: A comparison of Gulf Stream sea surface height fields derived from Geosat altimeter data and those derived from sea surface temperature data. *J. Atmos. Oceanic Technol.,* **10,** 76–87.

Glenn, S. M., D. L. Porter, and A. R. Robinson, 1991: A synthetic geoid validation of Geosat mesoscale dynamic topography in the Gulf Stream region. *J. Geophys. Res.,* **96,** 7145–7166.

Haines, K., 1991: A direct method for assimilating sea surface height data into ocean models with adjustment to the deep circulation. *J. Phys. Oceanogr.,* **21,** 843–868.

Holland, W. R., and P. Malanotte-Rizzoli, 1989: Assimilation of altimeter data into an ocean model: Space verses time resolution studies. *J. Phys. Oceanogr.,* **19,** 1507–1534.

Hurlburt, H. E., D. N. Fox, and E. J. Metzger, 1990: Statistical inference of weakly correlated subthermocline fields from satellite altimetry data. *J. Geophys. Res.,* **95,** 11 375–11 409.

Kelly, K. A., 1991: The meandering Gulf Stream as seen by the GEOSAT altimeter: Surface transport, position, and velocity variance from 73° to 46°W. *J. Geophys. Res.,* **96,** 16 721–16 738.

Kindle, J. C., 1986: Sampling strategies and model assimilation of

altimetric data for ocean monitoring and prediction. *J. Geophys. Res.,* **91,** 2418–2432.

Mellor, G. L., 1992: User's guide for a three-dimensional, primitive equation, numerical ocean model. Progress in Atmospheric and Oceanic Sciences Rep., Princeton University, 35 pp. [Available from Program in Atmospheric and Oceanic Sciences, Princeton University, Princeton, NJ 08544-0710.]

——, and T. Yamada, 1982: Development of a turbulent closure model for geophysical fluid problems. *Rev. Geophys.,* **20,** 851–875.

——, and T. Ezer, 1991: A Gulf Stream model and an altimetry assimilation scheme. *J. Geophys. Res.,* **96,** 8779–8795.

——, C. Mechoso, and E. Keto, 1982: A diagnostic calculation of the general circulation of the Atlantic Ocean. *Deep-Sea Res.,* **29,** 1171–1192.

Moore, A. M., 1991: Data assimilation in a quasi-geostrophic open-ocean model of the Gulf Stream region using the adjoint method. *J. Phys. Oceanogr.,* **21,** 398–427.

Oberhuber, J. M., 1988: An atlas based on the COADS data set: The budgets of heat, buoyancy and turbulent kinetic energy at the surface of the global ocean. Max-Planck Institut für Meteorologie Rep. 15, 196 pp.

Oey, L.-Y., T. Ezer, G. L. Mellor, and P. Chen, 1992: A model study of 'bump' induced western boundary current variabilities. *J. Mar. Syst.,* **3,** 321–342.

Pinardi, N., A. Rosati, and R. C. Pacanowski, 1995: The sea surface pressure formulation of rigid lid models. Implications for altimetric data assimilation studies. *J. Mar. Syst.,* **6,** 109–119.

Rienecher, M. M., and D. Adamec, 1995: Assimilation of altimeter data into a quasigeostrophic ocean model using optimal interpolation and EOFs. *J. Mar. Syst.,* **6,** 125–143.

Robinson, A. R., M. A. Spall, L. J. Walsted, and W. G. Leslie, 1989: Data assimilation and dynamic interpolation in Gulfcast experiments. *Dyn. Atmos. Oceans,* **13,** 301–316.

Thompson, J. D., and W. J. Schmitz, 1989: A limited-area model of the Gulf Stream: Design, initial experiments, and model-data intercomparison. *J. Phys. Oceanogr.,* **19,** 791–814.

Verron, J., 1992: Nudging satellite altimeter data into quasi-geostrophic ocean model. *J. Geophys. Res.,* **97,** 7479–7491.

White, W. B., C.-K. Tai, and W. R. Holland, 1990: Continuous assimilation of simulated GEOSAT altimetric sea level into an eddy-resolving numerical ocean model. 1. Sea level differences. *J. Geophys. Res.,* **95,** 3219–3234.

Willems, R. C., and Coauthors, 1994: Experiment evaluates ocean models and data assimilation in the Gulf Stream. *Eos, Trans. Amer. Geophys. Union,* **75,** 385–394.